CRYSTAL GROWTH & DESIGN

Article

pubs.acs.org/crystal

Control of Assembly of Dihydropyridyl and Pyridyl Molecules via Directed Hydrogen Bonding

Jian Lü,[†,‡] Li-Wei Han,[†,§] Nada H. Alsmail,[‡] Alexander J. Blake,[‡] William Lewis,[‡] Rong Cao,*[,†] and Martin Schröder*[,‡,∥]

[†]State Key Laboratory of Structural Chemistry, Fujian Institute of Research on the Structure of Matter, Chinese Academy of Sciences, Fuzhou, 350002 Fujian, P. R. China

[‡]School of Chemistry, University of Nottingham, University Park, Nottingham NG7 2RD, U.K.

[∥]School of Chemistry, University of Manchester, Manchester M13 9PL, U.K.

[§]School of Chemistry and Chemical Engineering, Nantong University, Nantong, 226019 Jiangsu, P. R. China

S *Supporting Information*

ABSTRACT: The crystallization of two dihydropyridyl molecules, 1,4-bis(4-(3,5-dicyano-2,6-dipyridyl)-dihydropyridyl)benzene ($[C_{40}H_{24}N_{10}]$·2DMF, **1**·2DMF; DMF = dimethylformamide) and 1,4-bis(4-(3,5-dicyano-2,6-dipyridyl)dihydropyridyl)phenylbenzene ($[C_{46}H_{28}N_{10}]$·2DMF, **3**·2DMF), and their respective oxidized pyridyl analogues, 1,4-bis(4-(3,5-dicyano-2,6-dipyridyl)pyridyl)-benzene ($[C_{40}H_{20}N_{10}]$, **2**) and 1,4-bis(4-(3,5-dicyano-2,6-dipyridyl)pyridyl)phenylbenzene ($[C_{46}H_{24}N_{10}]$·DMF, **4**·DMF), has been achieved under solvothermal conditions. The dihydropyridyl molecules are converted to their pyridyl products via in situ oxidative dehydrogenation in solution. The structures of the four molecules have been fully characterized by single crystal and powder X-ray diffraction. The oxidized pyridyl products, **2** and **4**, are more elongated due to aromatization of the dihydropyridyl rings at each end of their parent molecules **1** and **3**, respectively. The solid-state supramolecular structures of the pyridyl molecules are distinct from the dihydropyridyl molecules in terms of their hierarchical assembly via hydrogen bonding due to the loss of primary N−H hydrogen bond donors in the two electron oxidized tectons. Overall, the geometrically shorter molecules **1** and **3** display close-packed structures, whereas the more extended **2** and **4** assemble into more open supramolecular systems.

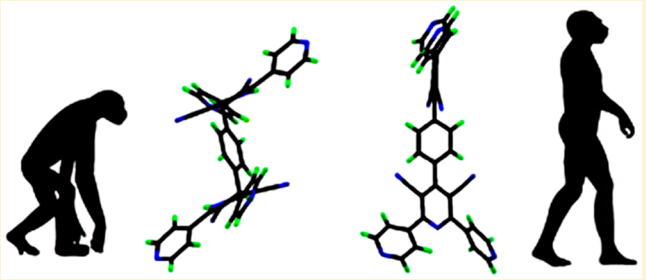

INTRODUCTION

Supramolecular organic assemblies, including single-component and multiple-component complexes, are a family of crystalline materials composed of molecular species held together in the solid state by long-range, noncovalent interactions.[1] The crystal engineering of organic assemblies is developing apace due to the increasing knowledge of the underlying supramolecular chemistry that directs the assembly and packing of molecules in the sold state. This defines their crystal structures and underpins the design and synthesis of new organic supramolecular materials,[2,3] which have found applications in a wide range of areas including host−guest recognition, proton conductivity, and gas adsorption and separations.[4,5] Among them, the hydrogen bonded supramolecular organic frameworks (SOFs, also referred to as HOFs (hydrogen bonded organic frameworks)) have received attention due to their design potential[5] and their structural and conceptual similarities to metal−organic frameworks (MOFs), which can also function as porous substrates/absorbent.[6] However, most hydrogen bonds are primarily electrostatic in nature and vary in strength according to the different donor and acceptor properties of functional groups and their environment, and thus prediction of structures of supramolecular organic arrays driven by hydrogen bonding can be challenging.[7] Predicting and understanding the packing of molecular assemblies is, therefore, a practical target toward the goal of designing and engineering solid-based materials.

Thermodynamically stable and crystalline supramolecular organic assemblies are most often prepared from the solutions using appropriate solvents through conventional crystallization under ambient conditions. In this context, some subtle factors, for example the acid−base properties of the solvent mixtures and the interaction of solvent molecules with the organic host, may be essential for the successful crystallization of the material in the solid state.[8] Moreover, in situ transformations of organic hosts have been observed,[9] and study of in situ transformations and their effect on resultant products and their relationship with precursors in terms of functional groups, supramolecular

Received: March 22, 2015
Revised: June 22, 2015
Published: July 28, 2015

DOI: 10.1021/acs.cgd.5b00395
Cryst. Growth Des. 2015, 15, 4219−4224

interactions, packing patterns, and order are of interest. We report herein the structures of four organic assemblies, 1,4-bis(4-(3,5-dicyano-2,6-dipyridyl)dihydropyridyl)benzene ([$C_{40}H_{24}N_{10}$]·2DMF, **1**·2DMF), 1,4-bis(4-(3,5-dicyano-2,6-dipyridyl)pyridyl)benzene ([$C_{40}H_{20}N_{10}$], **2**), 1,4-bis(4-(3,5-dicyano-2,6-dipyridyl)dihydropyridyl)phenylbenzene ([$C_{46}H_{28}N_{10}$]·2DMF, **3**·2DMF), and 1,4-bis(4-(3,5-dicyano-2,6-dipyridyl)pyridyl)phenylbenzene ([$C_{46}H_{24}N_{10}$]·DMF, **4**·DMF), in which **2** and **4** were prepared in situ from **1** and **3**, respectively, under solvothermal conditions (Scheme 1).

Scheme 1. Views of the Structures of the Dihydropyridyl and Pyridyl Tectons

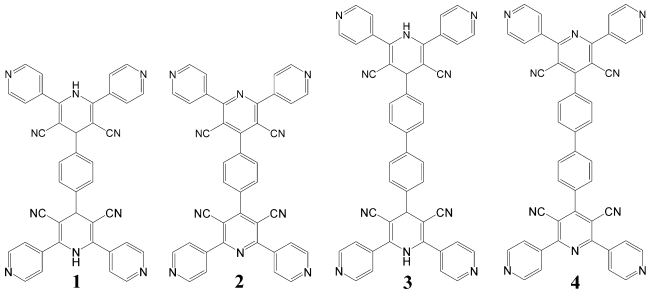

EXPERIMENTAL SECTION

Chemicals and General Methods. Commercially available reagents and organic solvents were used as received without further purification. Elemental analyses (C, H, and N) were carried out on an Elementar Vario EL III analyzer. Infrared (IR) spectra were recorded with a PerkinElmer Spectrum One as KBr pellets in the range 400−4000 cm^{-1}, and ^1H NMR spectra on a Bruker DPX-400 spectrometer. Thermal gravimetric analyses (TGA) were performed under a flow of N_2 (20 mL·min^{-1}) with a heating rate of 10 °C·min^{-1} using a TA SDT-600 thermogravimetric analyzer, and X-ray powder diffraction (PXRD) measurements were carried out at room temperature on a PANalytical X'Pert PRO diffractometer using Cu Kα radiation (λ = 1.5418 Å) at 40 kV, 40 mA, at a scan speed of 0.02°/s and a step size of 0.005° in 2θ.

Synthesis. *Synthesis of 3-Amino-3-(4-pyridinyl)propionitrile.* 4-Cyanopyridine (104 mg, 1.0 mmol), in MeCN (82 mg, 2.0 mmol), and potassium *tert*-butoxide (336 mg, 3.0 mmol) were added to toluene (40 mL), and the reaction mixture stirred at ambient temperature for 48 h. Saturated $NaHCO_3$ solution (200 mL) was used to quench the reaction, and the resultant solid crude product of 3-amino-3-(4-pyridinyl)propionitrile collected by filtrations, washed three times with NaCl solution, and dried in air. ^1H NMR (DMSO-d_6): 8.63 (d, J = 6.3 Hz, 2H, 2,6-pyridyl-H); 7.57 (d, J = 6.0 Hz, 2H, 3,5-pyridyl-H); 7.01 (s, 2H, NH), 4.4 (s, 1H, ═C−H) ppm. HRMS (EI-): m/z 439.0403 $[M + H]^+$. IR (KBr, ν_{max}, cm^{-1}): 2801 (w), 2759 (w), 2256 (m), 2194 (s), 1942 (m), 1670 (s), 1593 (s), 1530 (s), 1502 (s), 1425 (s), 1335 (m), 1271 (m), 1222 (m), 1146 (m), 1069 (m), 992 (s), 874 (m), 839 (s), 670 (s), 650 (s), 609 (s), 573 (s). Elemental analysis for $C_8H_7N_3$ (found/calcd): C, 66.15/66.19; H, 4.83/4.86; N, 28.94/28.95%.

Synthesis of 1,4-Bis(4-(3,5-dicyano-2,6-dipyridyl)dihydropyridyl)-benzene (1). 3-Amino-3-(4-pyridinyl)propionitrile (580 mg, 4.0 mmol) and 1,4-benzenedialdehyde (134 mg, 1.0 mmol) were added to glacial acetic acid (10 mL) which had been degassed for 10 min under N_2 flow. The reaction mixture was refluxed at 120 °C for 48 h, and the light yellow precipitate of **1** was collected by filtration, washed with hot acetic acid, EtOH, and distilled water, and dried in air. Crystals of **1**·2DMF suitable for single crystal X-ray diffractions were obtained by dissolving **1** (33 mg) in *N*,*N*-dimethylformamide (DMF) (3 mL) and slowly concentrating the solution by evaporation. ^1H NMR (DMSO-d_6): 10.41 (s, 2H, dihydropyridyl-NH), 8.76 (d, J = 5.9 Hz, 8H, Py-H), 7.70 (d, J = 4.7 Hz, 8H, Py-H); 7.65 (s, 4H, Ar-H), 4.90 (s, 2H, dihydropyridyl-CH) ppm. IR (KBr, ν_{max}, cm^{-1}): 2207 (s), 1641 (m), 1595 (m), 1545 (m), 1499 (s), 1406 (m), 1335 (m), 1289 (s), 1222 (w), 1193 (w), 1154 (w) 1068 (w), 987 (m), 830 (s). Elemental analysis for **1**·2DMF, $C_{46}H_{38}N_{12}O_2$ (found/calcd): C, 68.99/69.86; H, 4.27/4.84; N, 19.34/21.25%.

Synthesis of 1,4-Bis(4-(3,5-dicyano-2,6-dipyridyl)pyridyl)benzene (2). 50 mg of **1** was added to DMF (2 mL), sealed in a 15 mL pressure tube, and heated in an oil bath at 90 °C under autogenous pressure for 3 days. Colorless crystals of **2** suitable for single crystal X-ray diffraction were collected by filtration, washed with EtOH and distilled water, and dried in air. ^1H NMR (DMSO-d_6): 8.98 (d, J = 4.9 Hz, 8H, Py-H), 8.20 (s, 4H, Ar-H), 8.08 (d, J = 4.9 Hz, 8H, Py-H) ppm. IR (KBr, ν_{max}, cm^{-1}): 2207 (s), 1645 (m), 1595 (m), 1538 (m), 1499 (s), 1470 (m), 1413 (m), 1382 (m), 1289 (s), 1217 (w), 11893 (w), 1154 (w) 1125(w), 1062 (m), 994 (s), 834 (m), 803(s). Elemental analysis for **2**, $C_{40}H_{20}N_{10}.2H_2O$ (found/calcd): C, 71.02/71.00; H, 4.14/3.57; N, 20.47/20.69%.

Synthesis of 1,4-Bis(4-(3,5-dicyano-2,6-dipyridyl)dihydropyridyl)-phenylbenzene (3). **3** was prepared via a similar procedure to that of **1** but using 4,4′-biphenyldicarbaldehyde instead of benzene-1,4-benzenedicarbaldehyde. The light-yellow crystalline product of **3**·2DMF was collected by filtration, washed with hot acetic acid, EtOH, and distilled water, respectively, and dried in air. ^1H NMR (DMSO-d_6): 10.37 (s, 2H, dihydropyridyl-NH), 8.87−8.71 (m, 8H, Py-H), 7.87 (d, J = 8.2 Hz, 4H, Ar-H); 7.78−7.62 (m, 8H, Py-H; 4H, Ar-H), 4.93 (s, 2H, dihydropyridyl-CH) ppm. IR (KBr, ν_{max}, cm^{-1}): 2203 (s), 1648 (m), 1552 (w), 1513 (s), 1409 (m), 1346 (w), 1293 (m), 1218 (w), 1186 (w), 1150 (w) 1072 (w), 1005 (w), 880 (w), 827 (s). Elemental analysis for **3**·2DMF, $C_{55}H_{49}N_{13}O_3$ (found/calcd): C, 70.12/70.27; H, 4.54/5.25; N, 18.39/19.37%.

Synthesis of 1,4-Bis(4-(3,5-dicyano-2,6-dipyridyl)pyridyl)-phenylbenzene (4). **3** (50 mg) was added to DMF (2 mL), sealed in a 15 mL pressure tube, and heated in an oil bath at 90 °C under autogenous pressure for 3 days. Colorless crystals (**4**·DMF, suitable for single crystal X-ray diffraction) were collected by filtration, washed with EtOH and distilled water, respectively, and dried in air. IR (KBr, ν_{max}, cm^{-1}): 2235 (s), 1598 (m), 1559 (w), 1524 (s), 1488 (m), 1470 (m), 1414 (m), 1387 (s), 1325 (w) 1222 (w), 1193 (w), 1157 (w), 1126 (w), 1065 (m), 997 (m), 869 (w), 837 (s), 803 (s). Elemental analysis for **4**·2.5DMF, $C_{55}H_{45}N_{13}O_3$ (found/calcd): C, 71.13/71.44; H, 3.22/4.65; N, 19.56/19.46%.

Thermogravimetric Analyses (TGA). TGA plots of all four compounds are shown in Figure S2 in the Supporting Information. For compound **2**, which contains no solvent molecules in the crystal lattice, the weight loss observed after 320 °C corresponds to structural decomposition. For compounds **1**·2DMF, **3**·2DMF, and **4**·DMF, the first weight losses of 17.5%, 17.2%, and 9.1% before 130 °C are assigned to the loss of solvent DMF molecules (calculated ca. 18.4%, 16.8%, and 9.2%, respectively), followed by stability between 130 and 250 °C and followed by thermal decomposition. The number of solvent molecules associated with crystals of **1**−**4** has been determined by single crystal X-ray diffraction with electron densities calculated by the PLATON/SQUEEZE routine.[10] For bulk materials, where variability in solvent of crystallization was observed due to the synthesis and solvent volatility, a combination of TGA and elemental analysis was used.

X-ray Crystallography. Single crystal X-ray data for compounds **1**·2DMF, **2**, and **3**·2DMF were collected on Agilent SuperNova Atlas diffractometers, while the diffraction data for compound **4**·DMF was acquired using an Oxford Diffraction Xcalibur Eos instrument. The structure was solved by direct methods and developed by difference Fourier techniques, both using the SHELXL software package.[11] Hydrogen atoms of the ligands were placed geometrically and refined using a riding model. The unit cell volume of compounds **3** and **4** includes disordered solvent molecules (DMF) which could not be modeled as discrete atomic sites. We therefore employed PLATON/SQUEEZE[10] to calculate the contribution of the solvent region to the diffraction and thereby produced a set of solvent-free diffraction intensities. The solvent molecules of compounds **3** and **4** were not

DOI: 10.1021/acs.cgd.5b00395
Cryst. Growth Des. 2015, 15, 4219−4224

Table 1. Crystal Data and Structure Refinement for Compounds 1−4

	1	2	3	4
chem formula	$C_{46}H_{38}N_{12}O_2$	$C_{40}H_{20}N_{10}$	$C_{52}H_{42}N_{12}O_2$	$C_{49}H_{31}N_{11}O$
formula mass	790.88	640.66	866.97	789.94
cryst syst	monoclinic	monoclinic	monoclinic	orthorhombic
space group	$P2_1/c$	$C2/c$	$P2_1/c$	$Pbca$
a/Å	11.285(2)	34.345(3)	16.324(3)	7.6989(6)
b/Å	32.787(7)	9.2471(14)	6.8720(13)	27.8771(14)
c/Å	10.517(2)	10.6446(10)	21.928(4)	34.694(3)
α/deg	90	90	90	90
β/deg	98.979(4)	104.008(10)	101.657(3)	90
γ/deg	90	90	90	90
cell vol/Å^3	3843.6(14)	3280.1(7)	2409.1(8)	7446.1(9)
Z	4	4	2	8
reflns collected	21019	6837	12639	20302
indep reflns	7514	3227	4730	8630
R_{int}	0.0768	0.0298	0.0449	0.0486
final R_1 values ($I > 2\sigma(I)$)	0.0683	0.0561	0.0874	0.0757
final wR (F^2) values ($I > 2\sigma(I)$)	0.1565	0.1101	0.2565	0.1596
goodness of fit on F^2	1.014	1.030	1.012	0.972

included in the structural models but are included in the formulae. Carbon atoms on the central phenyl rings of **3** were treated as isotropic. CCDC 980607 (**1**), 980562 (**2**), 980572 (**3**), and 980586 (**4**) contain the supplementary crystallographic data for this paper. Data can be obtained free of charge from the Cambridge Crystallographic Data Centre via www.ccdc.cam.ac.uk/data_request/cif. A summary of the crystallographic data for compounds **1**−**4** is given in Table 1.

RESULTS AND DISCUSSION

The 1,4-bis-(4-(3,5-dicyano-2,6-dipyridyl)dihydropyridyl) derivatives (**1** and **3**, Scheme 1) were prepared from the reaction of 3-amino-3-(4-pyridinyl)propionitrile with 1,4-benzenedicarbaldehyde or 4,4′-biphenyldicarbaldehyde in glacial acetic acid at 120 °C, respectively. Solvothermal reactions of appropriate amount of **1** or **3** in *N*,*N*-dimethylformamide (DMF) yielded colorless crystalline solid of **2** or **4** in a yield of ca. 12%, and these products are insoluble in water and common organic solvents at room temperature. The structural transformation of **1** to **2** and **3** to **4** via oxidative dehydrogenation under solvothermal conditions has been confirmed by NMR spectroscopy and single crystal X-ray diffraction. The supramolecular chemistry of all four compounds has been comprehensively studied, and it has been found that the oxidative products, **2** and **4**, are somewhat elongated due to the aromatization of the dihydropyridyl rings located on each end of the parent molecules (**1** and **3**; Figure 1), Moreover, structures of **2** and **4** are distinct in that they are more linear than their parent zigzag dihdropyridyl parent molecules in terms of the hierarchical assemblies via hydrogen bonds.

Crystal Structures. **1**·2DMF crystallizes in monoclinic space group $P2_1/c$ with the asymmetric unit containing one 1,4-bis(4-(3,5-dicyano-2,6-dipyridyl)dihydropyridyl)benzene molecule and two solvent DMF molecules. A feature of **1** is that the two dihydropyridyl rings are nearly perpendicular (dihedral angle of ca. 83.34°) to the central phenyl ring as a result of the sp^3 carbon at the 4-position of each dihydropyridyl ring. Thus, molecules of **1** display zigzag configurations with the N−H groups on the dihydropyridyl rings expected to act as dominant hydrogen bond donors, and the *exo*-pyridyl and lateral cyano groups behaving as potential hydrogen bond acceptors. Each molecule of **1** interacts with two solvent DMF molecules via

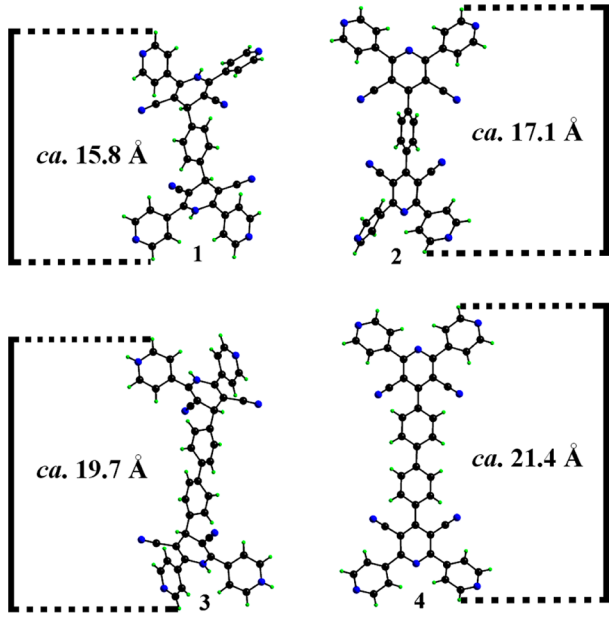

Figure 1. Comparison of the molecular sizes in compounds **1**−**4**.

hydrogen bonds from dihydropyridyl groups to amide groups (N−H···O interactions, 1.934(11) Å/1.971(15) Å; Table 2 and Table S1 in the Supporting Information). Two of the four *exo*-pyridyl groups of **1** interact with two neighboring ones via hydrogen bonds from phenyl groups to pyridyl groups (C−H···N interactions, 2.502(5) Å to 2.775(6) Å). Although DMF molecules block the connection of **1** to a neighboring molecule from the primary hydrogen bond donating sites, the pyridyl hydrogen bond accepting groups generate secondary C−H···N interactions and direct the assembly of **1** into a 2D hydrogen bonded square layer (Figure 2). A 3D supramolecular organic framework structure is thus formed through complex hydrogen bond and $\pi-\pi$ stacking interactions.

1,4-Bis(4-(3,5-dicyano-2,6-dipyridyl)pyridyl)benzene (**2**) crystallizes in the monoclinic space group $C2/c$. **2** possesses a linear central backbone with the two external pyridyl rings twisting around the central phenyl ring due to the rotation about C−C single bonds (torsion angles of 62.14° and 66.50°).

DOI: 10.1021/acs.cgd.5b00395
Cryst. Growth Des. 2015, 15, 4219−4224

Table 2. Selected Hydrogen Bond Lengths and Angles in Compounds 1−4

D	H	A	d(D−H)/Å	d(H−A)/Å	d(D−A)/Å	∠(D−H−A)/deg
			Compound **1**[a]			
N8	H8	O1#1	0.881(10)	1.934(11)	2.811(3)	173
N3	H3	O2#2	0.882(10)	1.971(15)	2.818(3)	161
			Compound **2**[b]			
C7	H7	N1#1	0.95	2.55	3.398(4)	148
			Compound **3**[c]			
N3	H3	N2#1	0.886(10)	2.019(14)	2.887(4)	166
C10	H10	N5#1	0.95	2.66	3.430(5)	138
C2	H2	N4#2	0.95	2.47	3.324(5)	149
			Compound **4**[d]			
C4	H4	N51	0.93	2.60	3.501(4)	164
C21	H21	N52	0.93	2.62	3.536(4)	171

[a]Compound **1**: #1: −1 + *x*, +*y*, +*z*. #2: 2 − *x*, 1 − *y* ,−*z*. [b]Compound **2**: #1: 1/2 − *x*, −1/2 + *y*, 1/2 − *z*. [c]Compound **3**: #1: 1 − *x*, −1/2 + *y*, 1/2 − *z*. #2: −*x*, −1/2 + *y*, 1/2 − *z*. [d]Compound **4**: #1: 3/2 − *x*, −*y*, 1/2 + *z*. #2: 1/2 + *x*, 1/2 − *y*, 1 − *z*.

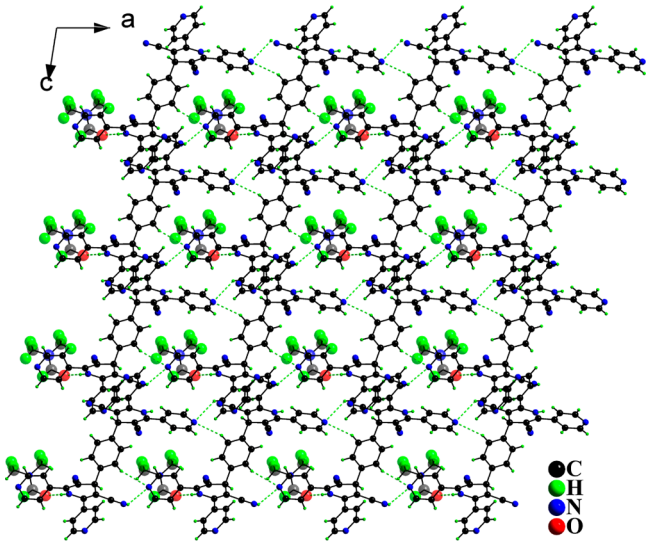

Figure 2. View of hydrogen bonded square layer structure of compound **1**. Guest DMF molecules are indicated with larger spheres for clarity.

2 lacks the primary N−H hydrogen bond donating groups unlike its precursor **1** due to the oxidation of dihydropyridyl groups, and thus the *exo*-pyridyl and lateral cyano hydrogen bond accepting groups interact mainly with the C−H groups of pyridyl or phenyl moieties (Table 2 and Table S1 in the Supporting Information). A 2D supramolecular network can be identified through hydrogen bond interactions from the pyridyl groups on the central backbones of **2** to the pyridyl/phenyl C−H groups of neighboring ones (Figure 3). The cyano groups decorate the 2D layers and interact with the C−H groups in the adjacent layers through C−H···N hydrogen bonds (Table 2 and Table S1 in the Supporting Information). Thus, a complex 3D supramolecular organic framework structure is formed through hydrogen bonding as well as $\pi-\pi$ stacking interactions between adjacent aromatic rings (pyridyl and/or phenyl).

The longer 1,4-bis(4-(3,5-dicyano-2,6-dipyridyl)-dihydropyridyl)phenylbenzene molecule (**3**) assembles into a 3D porous organic framework via hydrogen bonding. Single

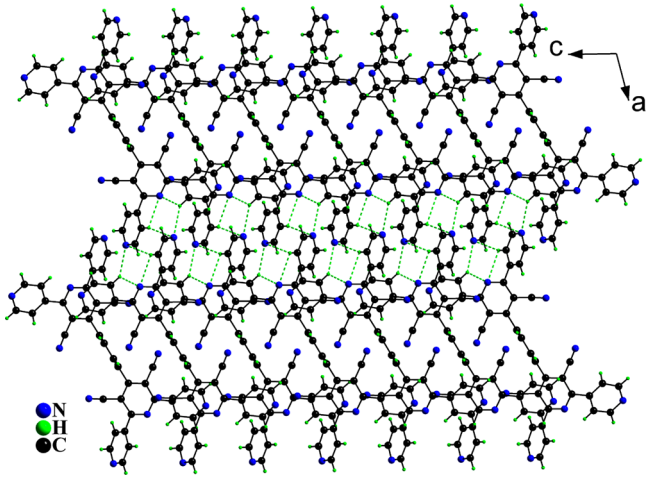

Figure 3. 2D hydrogen bonded layer structure in compound **2**.

crystal X-ray diffraction confirms that compound **3** crystallizes in monoclinic space group $P2_1/c$ and adopts a zigzag configuration due to the sp^3 carbon at the 4-position on each dihydropyridyl ring. The two central phenyl rings are coplanar and the two dihydropyridyl rings are nearly perpendicular to the central phenyl rings (dihedral angle of ca. 80.22°) similar to that of **1**. N−H groups on the dihydropyridyl rings of **3** participate in primary N−H···N hydrogen bond interactions (2.019(14) Å, Table 2 and Table S1 in the Supporting Information) with the pyridyl N atoms, which leads to the formation of a 2D hydrogen bonded square layer structure (Figure 4a). Secondary C−H···N interactions (Table 2 and Table S1 in the Supporting Information) between the lateral cyano and C−H groups on the skeleton of **3** account for the formation and stabilization of a 3D supramolecular organic framework with free pyridyl functional groups pointing toward the 1D channels along the crystallographic *b* axis (Figure 4b). The opening to these channels is estimated to be *ca.* 2.5 Å × 5.0 Å and the total solvent accessible volume of compound **3** after the removal of guest DMF molecules was estimated to be ca. 30%, calculated using PLATON/VOID routine.[10]

1,4-Bis(4-(3,5-dicyano-2,6-dipyridyl)pyridyl)phenylbenzene (**4**) crystallizes in the orthorhombic space group *Pbca* as **4**·DMF. Unlike **3**, the two phenyl rings of **4** are twisted from each other with a torsion angle of ca. 46.38° and the neighboring pyridyl rings have torsion angles of ca. 45.09° and 47.36° with respect to each phenyl ring. One molecule of **4** interacts with four others, two at each end via C−H···N interactions between the N-donors and C−H groups on the pyridyl rings (Figure 5, inset). In this way, a 3D supramolecular framework with 1D channels along the crystallographic *a* axis is formed (Figure 5). The opening of the channels is estimated to be 7.0 Å × 9.2 Å. In addition, **4** incorporates two identical 3D supramolecular nets that interpenetrate through each other with interactions observed through C−H···N hydrogen bonds (Table 2 and Table S1 in the Supporting Information). This framework interpenetration severely decreases the structural porosity to ca. 8% of solvent accessible volume in the solvent-free structure of **4** as confirmed by *PLATON/VOID* calculation.[10]

It has been found that **2** and **4** are longer than the parent molecules **1** and **3** (Figure 1) due to the oxidative dehydrogenation of the dihydropyridyl moieties to form pyridyl rings. The supramolecular structures of the four molecules have been interpreted in terms of their hydrogen bonded structures

DOI: 10.1021/acs.cgd.5b00395
Cryst. Growth Des. 2015, 15, 4219−4224

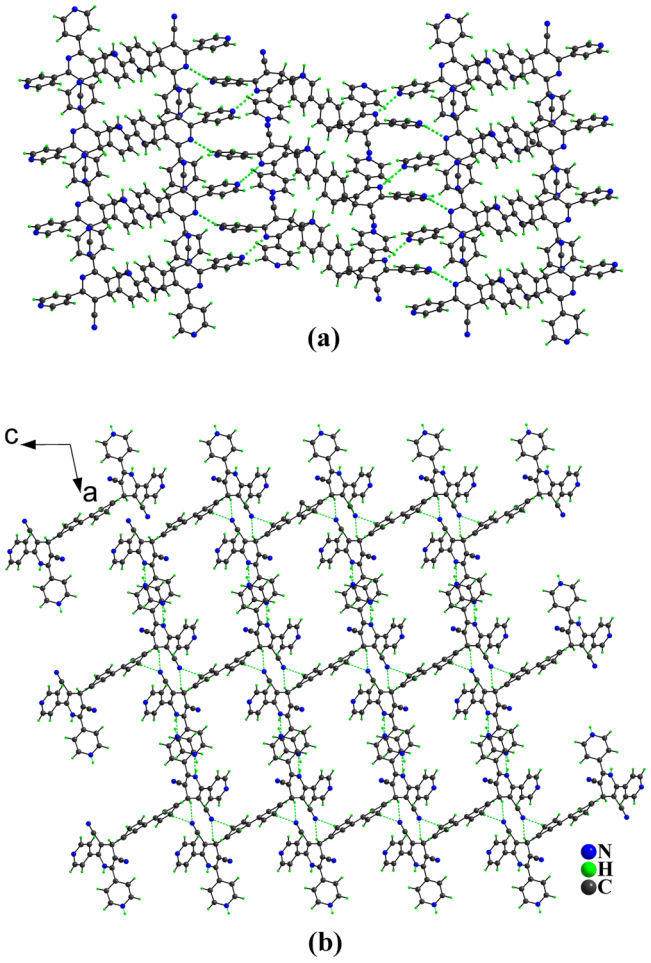

Figure 4. View of the 2D hydrogen bonded square layer structure in **3** (a) and 3D hydrogen bonded supramolecular organic framework in **3** (b).

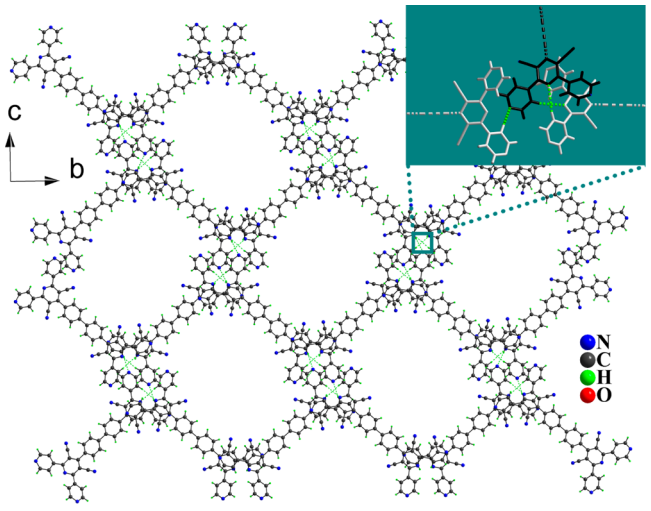

Figure 5. 2D hydrogen bonded honeycomb-like layer structure in compound **4**. Inset: a view of the hydrogen bonding interactions of **4**.

in the sold state. Among the multiple hierarchical hydrogen bonds which direct the self-assembly of the solvated compounds, N−H···A (A = N or O) appear to be the strongest amd most prevalent. Compounds **1** and **2** assemble into nonporous close-packed structures, whereas the biphenyl analogues, **3** and **4**, build into potential porous phases. The supramolecular structure of **3**·2DMF is reminiscent of the organic framework material **SOF-1** in which a similar molecular tecton with an extra central anthracene moiety was used.[5g] However, **3**·2DMF shows fairly poor framework stability on solvent exchange and desolvation, probably due to the lack of strong $\pi-\pi$ stacking interactions, which are observed in **SOF-1**, and we argue that it is these $\pi-\pi$ interactions that are responsible for the exceptionally high thermal stability of **SOF-1**. **4**·DMF possesses a promising porous 3D hydrogen bonded substructure; however, the observed framework interpenetration severely reduces the structural porosity. Thus, the balance between molecular size and topology of tectons and observed structural porosity of the resultant solid-state materials is crucial for the design and practical application of supramolecular organic assemblies.

CONCLUSIONS

In summary, the present work explores the supramolecular structures of two organic multiple-pyridyl derivatives, 1,4-bis(4-(3,5-dicyano-2,6-dipyridyl)dihydropyridyl)benzene (**1**) and 1,4-bis(4-(3,5-dicyano-2,6-dipyridyl)dihydropyridyl)-phenylbenzene (**3**), as well as the in situ formation of their elongated pyridyl analogues, 1,4-bis(4-(3,5-dicyano-2,6-dipyridyl)pyridyl)benzene (**2**) and 1,4-bis(4-(3,5-dicyano-2,6-dipyridyl)pyridyl)phenylbenzene (**4**). It has been shown the dihydropyridyl groups in **1** and **3** offer reliable hydrogen bond donating sites that give primary and strong hydrogen bonding interactions to O-/N-containing hydrogen bond acceptors; secondary C−H···N interactions are responsible for hierarchical assemblies of the overall supramolecular structures. The current research offers a possible route to the design of supramolecular organic assemblies from structural transformations of organic modules with similar functionalities. The structures of these organic solid materials are stabilized by hierarchical hydrogen bonds generated from more favorable functional groups.

ASSOCIATED CONTENT

Supporting Information

Additional figures of IR, TGA, and PXRD data and crystallographic data in CIF format. The Supporting Information is available free of charge on the ACS Publications website at DOI: 10.1021/acs.cgd.5b00395.

AUTHOR INFORMATION

Corresponding Authors

*E-mail: M.Schroder@manchester.ac.uk.
*E-mail: rcao@fjirsm.ac.cn.

Notes

The authors declare no competing financial interest.

ACKNOWLEDGMENTS

We thank EPSRC and the University of Nottingham for support. Financial support from the 973 Program (2011CB932504, 2012CB821705), NSFC (21331006, 21221001, 21101155, and 21203199), Fujian Key Laboratory of Nanomaterials (2006L2005), and Key Project from CAS are gratefully acknowledged. J.L. and M.S. thank the NSFC-RS for the International Exchanges Scheme (2011 China Costshare project based on NSFC 21001105) for financial support. J.L. acknowledges the Royal Society Sino-British Fellowship Trust for an Incoming Fellowship. N.H.A. thanks the Royal

DOI: 10.1021/acs.cgd.5b00395
Cryst. Growth Des. 2015, 15, 4219−4224

Commission for Jubail and Yanbu, Jubail University College, Kingdom of Saudi Arabia, for a PhD Scholarship. M.S. gratefully acknowledges receipt of an ERC Advanced Grant. We thank a referee for helpful comments on the crystallographic analysis of these compounds.

REFERENCES

(1) (a) Desiraju, G. R.; Vittal, J. J.; Ramanan, A. *Crystal Engineering: A Textbook*; World Scientific Publishing: Singapore, 2011. (b) Burrows, A. D. *Struct. Bonding (Berlin)* **2004**, *108*, 55. (a) Lee, T.; Wang, P. Y. *Cryst. Growth Des.* **2010**, *10*, 1419. (b) Oliveira, M. A.; Peterson, M. L.; Klein, D. *Cryst. Growth Des.* **2008**, *8*, 4487. (c) Bis, J. A.; Vishweshwar, P.; Middleton, R. A.; Zaworotko, M. J. *Cryst. Growth Des.* **2006**, *6*, 1048. (d) Comotti, A.; Bracco, S.; Ben, T.; Qiu, S.; Sozzani, P. *Angew. Chem., Int. Ed.* **2014**, *53*, 1043. (e) Comotti, A.; Bracco, S.; Yamamoto, A.; Beretta, M.; Hirukawa, T.; Tohnai, N.; Miyata, M.; Sozzani, P. *J. Am. Chem. Soc.* **2014**, *136*, 618. (f) Muller, T.; Bräse, S. *RSC Adv.* **2014**, *4*, 6886.

(2) (a) Vishweshwar, P.; McMahon, J. A.; Bis, J. A.; Zaworotko, M. J. *J. Pharm. Sci.* **2006**, *95*, 499. (b) Vishweshwar, P.; McMahon, J. A.; Peterson, M. L.; Hickey, M. B.; Shattock, T. R.; Zaworotko, M. J. *Chem. Commun.* **2005**, 4601. (c) Almarsson, Ö.; Zaworotko, M. J. *Chem. Commun.* **2004**, 1889. (d) Distefano, G.; Comotti, A.; Bracco, S.; Beretta, M.; Sozzani, P. *Angew. Chem., Int. Ed.* **2012**, *51*, 9258. (d) Xiao, B.; Easun, T. L.; Dhakshinamoorthy, A.; Cebula, I.; Beton, P. H.; Titman, J. J.; Garcia, H.; Thomas, K. M.; Schröder, M. *J. Mater. Chem. A* **2014**, *2*, 19889.

(3) (a) Khan, M.; Enkelmann, V.; Brunklaus, G. *J. Am. Chem. Soc.* **2010**, *132*, 5254. (b) Kirchner, M. T.; Bläser, D.; Boese, R. *Chem. - Eur. J.* **2010**, *16*, 2131. (c) Anderson, K. M.; Probert, M. R.; Whiteley, C. N.; Rowland, A. M.; Goeta, A. E.; Steed, J. W. *Cryst. Growth Des.* **2009**, *9*, 1082. (d) Bhatt, P. M.; Azim, Y.; Thakur, T. S.; Desiraju, G. R. *Cryst. Growth Des.* **2009**, *9*, 951. (e) Stanton, M. K.; Bak, A. *Cryst. Growth Des.* **2008**, *8*, 3856. (f) Childs, S. L.; Chyall, L. J.; Dunlap, J. T.; Smolenskaya, V. N.; Stahly, B. C.; Stahly, P. G. *J. Am. Chem. Soc.* **2004**, *126*, 13335. (g) Remenar, J. F.; Morissette, S. L.; Peterson, M. L.; Moulton, B.; MacPhee, J. M.; Guzman, H. R.; Almarsson, Ö. *J. Am. Chem. Soc.* **2003**, *125*, 8456. (h) Fleischman, S. G.; Kuduva, S. S.; McMahon, J. A.; Moulton, B.; Bailey Walsh, R. D.; Rodriguez-Hornedo, N.; Zaworotko, M. J. *Cryst. Growth Des.* **2003**, *3*, 909. (i) Ling, I.; Alias, Y.; Sobolev, A. N.; Raston, C. L. *New J. Chem.* **2010**, *34*, 414. (j) Martin, A. D.; Hartlieb, K. J.; Sobolev, A. N.; Raston, C. L. *Cryst. Growth Des.* **2010**, *10*, 5302.

(4) (a) Cooper, A. I. *Angew. Chem., Int. Ed.* **2012**, *51*, 7892. (b) Hasell, T.; Chong, S. Y.; Jelfs, K. E.; Adams, D. J.; Cooper, A. I. *J. Am. Chem. Soc.* **2012**, *134*, 588. (c) Bojdys, M. J.; Briggs, M. E.; Jones, J. T. A.; Adams, D. J.; Chong, S. Y.; Schmidtmann, M.; Cooper, A. I. *J. Am. Chem. Soc.* **2011**, *133*, 16566. (d) Hasell, T.; Schmidtmann, M.; Cooper, A. I. *J. Am. Chem. Soc.* **2011**, *133*, 14920. (e) Tian, J.; Ma, S.; Thallapally, P. K.; Fowler, D.; McGrail, B. P.; Atwood, J. L. *Chem. Commun.* **2011**, *47*, 7626. (f) Kim, H.; Kim, Y.; Yoon, M.; Lim, S.; Park, S. M.; Seo, G.; Kim, K. *J. Am. Chem. Soc.* **2010**, *132*, 12200. (g) Lim, S.; Kim, H.; Selvapalam, N.; Kim, K.-J.; Cho, S. J.; Seo, G.; Kim, K. *Angew. Chem., Int. Ed.* **2008**, *47*, 3352.

(5) (a) Lü, J.; Perez-Krap, C.; Suyetin, M.; Alsmail, N. H.; Yan, Y.; Yang, S.; Lewis, W.; Bichoutskaia, E.; Tang, C. C.; Blake, A. J.; Cao, R.; Schröder, M. *J. Am. Chem. Soc.* **2014**, *136*, 12828. (b) Luo, X.-Z.; Jia, X.-J.; Deng, J.-H.; Zhong, J. L.; Liu, H. J.; Wang, K. J.; Zhong, D.-C. *J. Am. Chem. Soc.* **2013**, *135*, 11684. (c) Li, P.; He, Y.; Guang, J.; Weng, L.; Zhao, J. C.-G.; Xiang, S.; Chen, B. *J. Am. Chem. Soc.* **2014**, *136*, 547. (d) Yamamoto, A.; Hamada, T.; Hisaki, I.; Miyata, M.; Tohnai, N. *Angew. Chem., Int. Ed.* **2013**, *52*, 1709. (e) Mastalerz, M.; Oppel, I. M. *Angew. Chem., Int. Ed.* **2012**, *51*, 5252. (f) He, Y.; Xiang, S.; Chen, B. *J. Am. Chem. Soc.* **2011**, *133*, 14570. (g) Yang, W.; Greenaway, A.; Lin, X.; Matsuda, R.; Blake, A. J.; Wilson, C.; Lewis, W.; Hubberstey, P.; Kitagawa, S.; Champness, N. R.; Schröder, M. *J. Am. Chem. Soc.* **2010**, *132*, 14457. (h) Sozzani, P.; Bracco, S.; Comotti, A.; Ferretti, L.; Simonutti, R. *Angew. Chem., Int. Ed.* **2005**, *44*, 1816. (i) Zhang, G.; Presly, O.; White, F.; Oppel, I. M.; Mastalerz, M. *Angew. Chem., Int. Ed.* **2014**, *53*, 5126. (j) Zhang, G.; Presly, O.; White, F.; Oppel, I. M.; Mastalerz, M. *Angew. Chem., Int. Ed.* **2014**, *53*, 1516.

(6) (a) Lin, X.; Champness, N. R.; Schröder, M. *Top. Curr. Chem.* **2010**, *293*, 35. (b) Sumida, K.; Rogow, D. L.; Mason, J. A.; McDonald, T. M.; Bloch, E. D.; Herm, Z. R.; Bae, T.-H.; Long, J. R. *Chem. Rev.* **2012**, *112*, 724. (c) Makal, T. A.; Li, J.-R.; Lu, W.; Zhou, H.-C. *Chem. Soc. Rev.* **2012**, *41*, 7761.

(7) For example see: (a) Bhogala, B. R.; Nangia, A. *New J. Chem.* **2008**, *32*, 800. (b) Chiarella, R. A.; Davey, R. J.; Peterson, M. L. *Cryst. Growth Des.* **2007**, *7*, 1223. (c) Aakeröy, C. B.; Desper, J.; Scott, B. M. T. *Chem. Commun.* **2006**, 1445.

(8) Aakeröy, C. B.; Rajbanshi, A.; Li, Z. J.; Desper, J. *CrystEngComm* **2010**, *12*, 4231.

(9) (a) Lü, J.; Han, L.-W.; Lin, J.-X.; Cao, R. *Cryst. Growth Des.* **2011**, *11*, 2035. (b) Ning, S.; Toda, F.; Jones, W. *CrystEngComm* **2009**, *11*, 375. (c) Shan, N.; Toda, F.; Jones, W. *Chem. Commun.* **2002**, 2372. (d) Toda, F. *Acc. Chem. Res.* **1995**, *28*, 480.

(10) Spek, A. L. *Acta Crystallogr., Sect. D: Biol. Crystallogr.* **2009**, *65*, 148.

(11) Sheldrick, G. M. SHELXS97. *Acta Crystallogr., Sect. A: Found. Crystallogr.* **2008**, *64*, 112.

DOI: 10.1021/acs.cgd.5b00395
Cryst. Growth Des. 2015, 15, 4219−4224